applied sciences

MDPI

Review

Line-Shaped Illumination: A Promising Configuration for a Flexible Two-Photon Microscopy Setup

Jacopo Parravicini [1,2,3,*], Elton Hasani [4,5] and Luca Tartara [4]

[1] Dipartimento di Fisica & Astronomia, Università di Firenze, IT-50019 Sesto Fiorentino, FI, Italy
[2] LENS—European Laboratory for Nonlinear Spectroscopy, IT-50019 Sesto Fiorentino, FI, Italy
[3] INO-CNR—Istituto Nazionale di Ottica del Consiglio Nazionale delle Ricerche, IT-50019 Sesto Fiorentino, FI, Italy
[4] Dipartimento di Ingegneria Industriale e dell'Informazione, Università di Pavia, IT-27100 Pavia, PV, Italy; eltonhasani@gmail.com (E.H.); tartara@unipv.it (L.T.)
[5] Bright Solutions, IT-27100 Cura Carpignano, PV, Italy
* Correspondence: jacopo.parravicini@unifi.it; Tel.: +39-055-457-2308

Featured Application: Two-photon microscopy imaging, real-time two-photon imaging, nonlinear spectral measurements, dye characterization, biological sample imaging.

Abstract: An innovative two-photon microscope exploiting a line-shaped illumination has been recently devised and then implemented. Such configuration allows to carry out a real-time detection by means of standard CCD cameras and is able to maintain the same resolution as commonly used point-scanning devices, thus overcoming what is usually regarded as the main limitation of line-scanning microscopes. Here, we provide an overview of the applications in which this device has been tested and has proved to be a flexible and efficient tool, namely imaging of biological samples, in-depth sample reconstruction, two-photon spectra detection, and dye cross-section measurements. These results demonstrate that the considered setup is promising for future developments in many areas of research and applications.

Keywords: two-photon microscopy; two-photon absorption; imaging technique; experimental technique; nonlinear spectra; dyes

Citation: Parravicini, J.; Hasani, E.; Tartara, L. Line-Shaped Illumination: A Promising Configuration for a Flexible Two-Photon Microscopy Setup. *Appl. Sci.* **2022**, *12*, 3938. https://doi.org/10.3390/app12083938

Academic Editors: Vibhav Bharadwaj and Sanathana Konugolu Venkata Sekar

Received: 21 February 2022
Accepted: 11 April 2022
Published: 13 April 2022

1. Introduction

Nonlinear fluorescence microscopy is widely recognized as an important and consolidated technique to investigate biological samples. In most cases, this approach relies on two-photon excited fluorescence (TPEF), which exploits two-photon absorption (TPA) and consequent fluorescence emission to obtain images, especially of biological samples [1]. This method has several advantages, such as great penetration depth, high longitudinal resolution, suitability for three-dimensional image reconstruction, low phototoxicity, and low photobleaching effects [2–5]. However, a specific drawback of this technique is that generally, real-time imaging (at least 30 frames per second) is not available: the acquisition of a two-dimensional image usually requires several seconds, so that the possible reconstruction of a three-dimensional image from a stack of in-plane images may take minutes, a time range which is too long for several applications [1]. Moreover, quite expensive and tricky single-photon counters are often required as detectors, with the consequent need for complex driving electronics [6,7]. Although many approaches have been devised to solve this issue, up until now, no satisfying solutions have achieved the necessary reliability to be exploited in commercial instruments [6]. In principle, the increase of the acquisition rate can be obtained by exploiting a multifocal configuration, in which several focal points are generated in the sample at a time. Line-shaped illumination is the most straightforward configuration to obtain this multifocal pattern: the light beam emitted by the illuminating

laser is first shaped by means of cylindrical lenses and is focused inside the sample with a continuous line, as shown in Figure 1. The simultaneous excitation of several points in the specimen is expected to reduce the acquisition time, as a two-dimensional image is obtained by scanning the line along a single direction. As a consequence, a N × N-pixel image would require a number of acquisitions reduced by a factor of N. The time for the reconstruction of a three-dimensional image would then be strongly decreased as well. Nevertheless, past experimental works showed that such an approach would strongly worsen the axial resolution with respect to point-scanning microscopes. Namely, Guild et al. pointed out that, contrarily to the TPEF in a point-scanning configuration, the total line-focused TPEF increases logarithmically with the thickness of the sample, so that the additional spurious fluorescence reaches twice the signal level generated in the focal volume for a thickness of about 100 μm [8]. On the other hand, Brakenhoff et al. evaluated the worsening of the sectioning capability in comparison to point-focused TPEF as 5 μm with respect to 1 μm [4,9]. Although some solutions have been devised to overcome this drawback, which in principle could provide roughly the same resolution of a point-scanning system, none of them have spread out among applications yet [10]. Particularly, in [10], a 1.5 μm resolution has been obtained by means of temporal focusing.

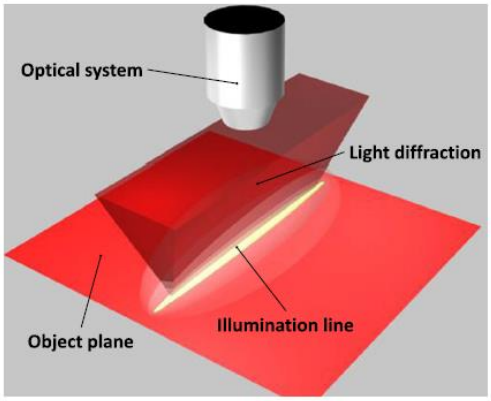

Figure 1. Adapted from [11]: ideal scheme of the considered problem.

In recent years, an innovative line-scanning TPEF microscopy configuration has been proposed [12]. Actually, theoretical calculations have shown that a line-shaped illumination is able to afford an axial resolution comparable to that obtained by a point-shaped illumination, provided that the optical elements are properly arranged [11]. Indeed, the proposed setup exploits a relatively simple optical configuration, only using standard spherical and cylindrical lenses, nonetheless obtaining an optimized performance in terms of resolution. Such approach for a *line-scanning two-photon microscope* (LSTPM) allows us to obtain both the acquisition of images at video rate and the suppression of the resolution degradation, which is usually found in line-scanning systems. A specific feature of the proposed setup is the large flexibility in applications. Indeed, until now, it has been experimentally demonstrated to be a good tool for measurements of two-photon absorption spectra and cross-sections [13,14], as well as for imaging of several kinds of biological samples and for their in-depth image reconstruction [14–17].

In this review paper, we first describe the proposed and experimentally realized microscope setup, and then we provide an overview of the main results by discussing the applications in which the technique has already been fruitfully validated.

2. Description of the Experimental Setup

The idea behind the proposed microscope setup arises from an exhaustive review of the scientific literature about line-scanning microscopes, in order to investigate the worsening of the resolution in comparison to point-scanning systems in detail. The reason is usually ascribed to the weak focusing, which occurs in only one of the two transverse

directions rather than to the astigmatism due to the cylindrical optics used for beam shaping. However, according to numerical simulations that we have performed, we have come to the conclusion that the role of such astigmatism is severely underestimated. Indeed, if the two focal volumes generated by the microscope objective both lie inside the sample, two contributions of nonlinear fluorescence to the detected signal will be generated, at two different depths, thus leading to a degradation of the axial resolution. Moreover, if the separation between the two focal planes is small, the intensity of the excitation beam can be high enough to generate nonlinear fluorescence in all the regions in between. The microscope setup has then been designed so that the focal distance of one of the two planes is made infinite by collimating the beam out of the microscope objective in one of the two transverse directions. In such a way, the sectioning capability of the microscope is expected to be preserved, notwithstanding the linear focusing. This is possible by means of a proper arrangement of the lenses used in the optical system, which has not been considered in previous works [12,13]. As for the excitation intensity along the focal line, a uniform light distribution is highly desirable in order to yield a high in-plane resolution. In fact, if the intensity varies along the line, the power level being necessary to excite a detectable amount of nonlinear fluorescence in the low-intensity regions could possibly saturate the nonlinear absorption in the high-intensity regions, thus worsening the transverse resolution. As the beam emitted by a typical excitation laser source has a Gaussian shape, common cylindrical lenses generate a bell-shaped intensity distribution along the focal line. In order to avoid that, the most straightforward solution is the overfilling of the entrance pupil of the objective, so that the apodization of the beam will limit the intensity variations. Besides the residual unbalance in the intensity distribution, this approach would clearly suffer from an inefficient use of the laser power. A more efficient and better-performing solution can be obtained by means of a Powell lens, which is able to convert a Gaussian beam into a flat-top rectangular intensity distribution by fanning out an input collimated beam in one dimension. The design of the microscope turns out to be more complex, but the benefit in terms of performance appears to be appealing.

The excitation light source employed in the development of the LSTPM setup is a continuous-wave, mode-locked Ti:Sapphire laser (Tsunami, Spectra Physics), emitting femtosecond pulses at the repetition rate of 82 MHz. The beam has a full-width half-maximum diameter of 2 mm and is magnified by a factor of 1.5 by a Keplerian telescope before entering the microscope setup, which is shown in Figure 2. As the beam profile is Gaussian, a Powell lens with a fun angle of 20° is used in order to yield a flat-top profile in one of the two transverse directions. In such direction, the beam turns out to be highly divergent and it is subsequently recollimated by means of a 25 mm focal length cylindrical lens, thus making up an effective Galilean expander.

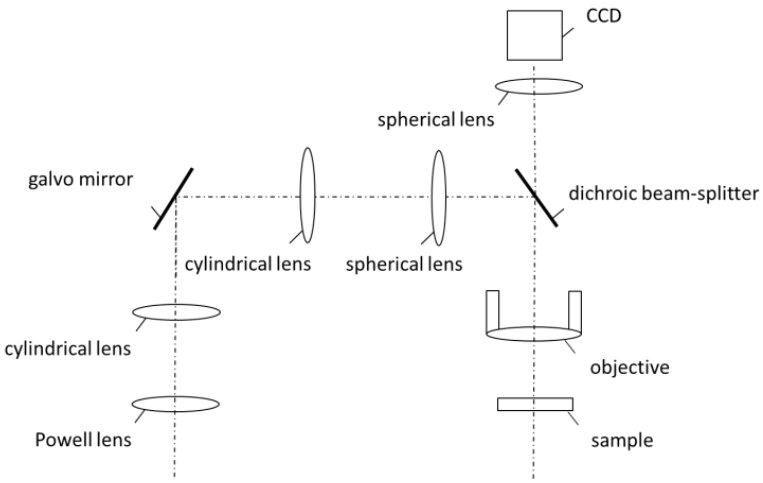

Figure 2. Microscope setup.

The beam then impinges on a single-axis galvanometer scan mirror providing deflection along the perpendicular direction at a maximum angle of 25°. A pair of a 50 mm focal length cylindrical lenses acting in the scan direction and a confocally arranged 100 mm focal length spherical lens relay the linear beam, having the desired uniform intensity distribution, on the entrance pupil of the objective after reflection by a dichroic beam-splitter. The microscope objective is confocally arranged with respect to the spherical lens, so that the emerging beam is collimated in the direction perpendicular to the scan direction. In such a way, the length of the line-shaped beam is kept fixed along the propagation inside the sample, thus allowing a precise control of the intensity. This makes it possible to set the input power to the proper level which is required to excite fluorescence just in the one focal plane lying at a finite distance [13,14].

Different objectives are employed according to the specimen under investigation and the associated required field of view. Usually, either a 60× or a 100× oil immersion objective is employed. The overall loss of the microscope setup is about 24%, with the main contribution arising from apodization of the beam after the Powell lens in order to trim the two intensity peaks at the ends. The sample is mounted on a three-axis translation stage, whose axial displacement is provided by a piezoelectric motor driven by a closed loop control system with a 20 nm resolution. In the transverse plane manual, translation stages provide a raw alignment of the sample with a resolution of 10 μm. The TPEF radiation is collected by the same objective, transmitted by the dichroic beam-splitter and a set of high-pass filters, and finally imaged in real time on the CCD camera (CoolSNAP EZ, Photometrics) by means of a tube lens (Figures 3 and 4a). The images are acquired by the open-source μManager software, which is a valuable tool for their eventual processing. Detailed information about μManager can be found in [18,19].

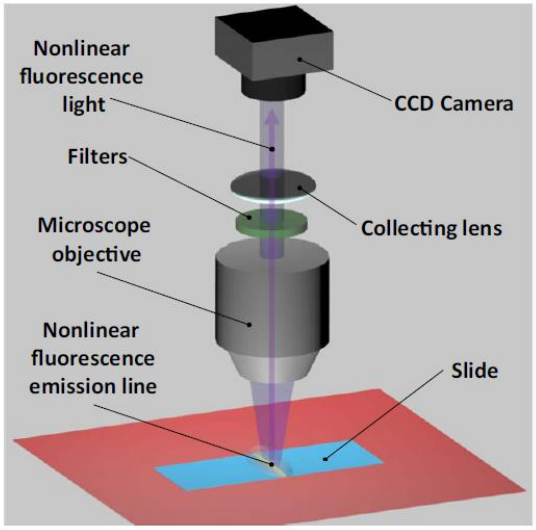

Figure 3. Adapted from [13]. Details of the detection part of the microscope scheme reported in Figure 2. Reproduced with permission from the authors, J. Opt.; published by IOP, 2016.

Particularly, the deconvolution with the spread function of the imaging system (Figure 4) is well-known to improve contrast and sharpness [1,11]. As in our microscope setup the illumination is shaped as a line, the so-called line-spread function is required. In the literature, the computation of such function is commonly performed by treating the line as an array of points. First, the point-spread function of each element of the array is evaluated by means of Bessel functions, and then an integration of the results along the direction of the line is performed, leading to the estimation of the line-spread function. As this computation is usually time-consuming because of the use of Bessel functions, we have proposed and validated a novel method which is based on the separate evaluation of the beam propagation along the two transverse directions. Indeed, the line-shaped beam will

diffract in the direction perpendicular to the line, but not in the direction of the line itself. It is thus possible to study the propagation under the Fresnel approximation in the former direction and under the Fraunhofer approximation in the latter, and finally to combine the results in order to obtain the line-spread function of the whole system. We have thus named this technique *the transversal direction decoupling method*. A detailed explanation can be found in [11].

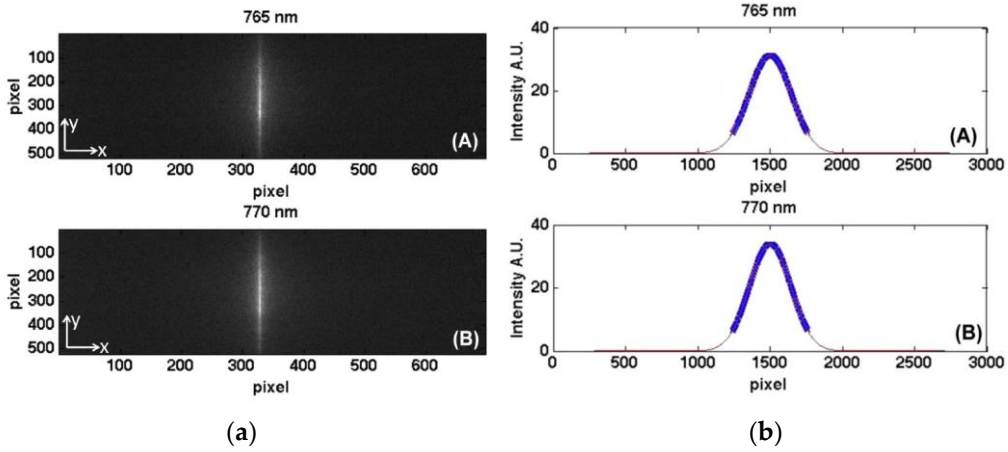

(**a**) (**b**)

Figure 4. Adapted from [13]. (**a**) Two-photon fluorescence emission generated by illumination lines at 765 (**A**) and 770 nm (**B**). (**b**) Two-photon fluorescence emission profile in y direction generated by 765 (**A**) and 770 nm (**B**) excitation wavelengths: measured intensity (blue crosses) and relative Gaussian fit (pink lines). In both panels, each pixel corresponds to 0.214 μm. Reproduced with permission from the authors, J. Microsc.; published by Wiley, 2018.

3. Overview of Applications

The LSTPM has been used for different purposes, demonstrating the reliability of the proposed experimental approach in different fields of research. As mentioned above, the technique has been tested for the characterization of dyes, namely two-photon spectral and cross-section measurements, and for imaging, namely investigation of biological samples and in-depth sample image reconstruction. Here, we provide an overview of such works.

3.1. Two-Photon Spectral Measurements

Several procedures have been devised for the measurement of TPA spectra. The technique exploiting the LSTPM setup belongs to the class of the so-called indirect methods [7,20]. The use of a line-shaped excitation light beam enables to obtain a high signal level, which is usually very difficult to obtain in two-photon fluorescence measurements (Sutherland2003). Here, we recall the basic steps of the proposed technique, while details of TPA spectra measurements by LSTPM are listed and discussed in [13]. The nonlinear fluorescence emission is measured for different values of the excitation wavelength. The TPEF optical power, $P_F(\lambda)$, as a function of the illumination wavelength, λ, is given by [1,2]:

$$P_F(\lambda) \propto \frac{\sigma(\lambda)}{\tau_p f_p} \left(\frac{\lambda}{hc}\right)^2 I_{av}^2 \quad (1)$$

where $\sigma(\lambda)$ is the TPA cross-section, τ_p is the pulse duration, f_p is the laser repetition rate, NA is the numerical aperture of the optical system focusing the laser beam on the sample (e.g., a microscope objective), h is the Planck constant, c is the speed of light in the vacuum, while $I_{av} = I_{av}(x, y)$ is the time-averaged illumination intensity distribution in the focal plane. If $I_F = I_F(x, y)$ is the fluorescence intensity distribution in the sample and A is the fluorescing area, the fluorescence emission, P_F, will be written as:

$$P_F = \int_A I_F(x,y)dxdy \quad (2)$$

The use of the LSTPM in order to measure TPA spectra is based on the calculation of the fluorescence response, $P_F = P_F(\lambda)$, as provided by Equation (2). In our approach, the fluorescence emission pattern $I_F = I_F(x, y)$ is detected by a CCD camera. P_F can then be retrieved from the geometry of the optical setup. Finally, $\sigma(\lambda)$ is obtained, except for a numerical constant, so that a relative TPA spectrum is obtained. Great care has to be taken about the spectral behavior of the optical components of the setup in order to minimize errors arising from wavelength-dependent properties. The spectral response of each element has thus been systematically tested by means of an optical spectrum analyzer (Ando AQ-6315). The response has proven to be flat for the wavelength range of the measurements with an error of 0.5%. Actually, this technique has been validated with dyes whose TPA spectra are available in the literature, i.e., fluorescein isothiocyanate (FITC) and Alexa 488 [13,14]. Comparisons between the spectra measured by LSTPM and those reported in the literature are shown in Figures 5 and 6, highlighting the very good performance of our novel technique in providing relative measurements.

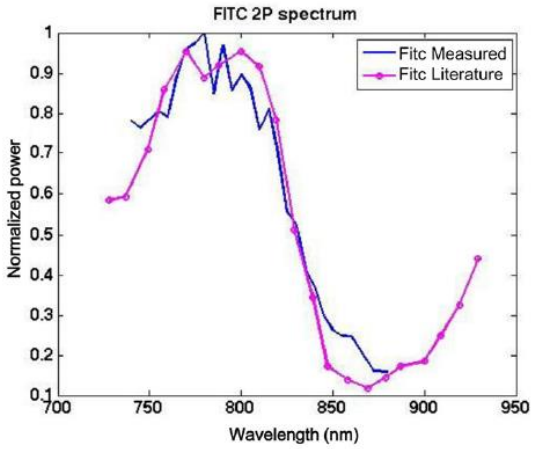

Figure 5. Adapted from [13]. Comparison between the two-photon absorption spectrum of FITC dextran from measurements (blue curve) and from the literature (fuchsia curve). Reproduced with permission from the authors, J. Microsc.; published by Wiley, 2018.

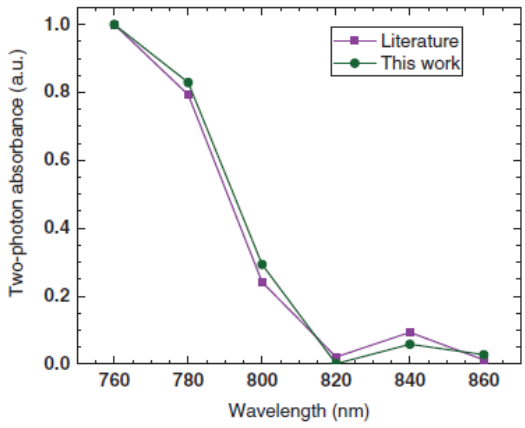

Figure 6. Adapted from [14]. Comparison between the two-photon absorption spectrum of Alexa 488 from measurements (green curve) and from the literature (violet curve). Reproduced with permission from the authors, J. Biophotonics.; published by Wiley, 2020.

We note that this method has the advantage of the intrinsic high selectivity on the TPA signal, which is a specific feature of the fluorescence-exploiting techniques. Moreover, a line-shaped beam allows to excite a large volume of the specimen, thus generating a strong two-photon fluorescence signal, which does not require a photon counter device to be recorded. Therefore, we can conclude that this approach has the advantage of employing an

experimental setup which is easier in comparison to other methods used for the estimation of nonlinear fluorescence.

3.2. Two-Photon Cross-Sections

The above-described technique exploiting LSTPM to measure nonlinear fluorescence spectra of dyes has been extended to obtain absolute measurements of the two-photon cross-section as a function of wavelength. In a pioneering work, two dyes which are commonly used for staining in standard white-light microscopy, eosin and hematoxylin, have been investigated [14]. First, their relative TPA spectra have been measured following the procedure described in the previous section. They are compared to the corresponding one-photon absorption spectra in Figure 7.

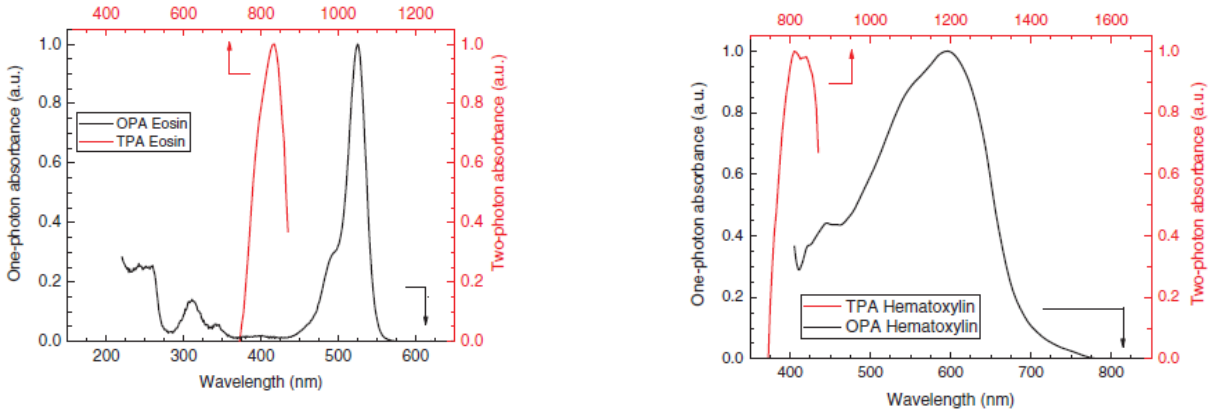

Figure 7. Adapted from [14]. (**a**) Comparison between the one-photon absorption spectrum (OPA, black) from the literature and the measured two-photon absorption spectrum (TPA, red) for eosin. (**b**) Comparison between the one-photon absorption spectrum (OPA, black) from the literature and the measured two-photon absorption spectrum (TPA, red) for hematoxylin. Reproduced with permission from the authors, J. Microsc.; published by Wiley, 2018.

The absolute values of the cross-sections provided in GM units were then evaluated by comparison to a dye with a known cross-section, following the procedure detailed in [14]. The TPA spectrum of Alexa 488 displayed in Figure 6 and the corresponding numerical values of the cross-section, which are available in the literature [21], are assumed as the reference data. Particularly, the cross-section of eosin was estimated from the ratio of the values of the measured fluorescence intensity. The data were rescaled by the ratio of the quantum yields and concentrations of the two dyes, which were assumed to be equal for the one-photon and the two-photon processes [22]. On the other hand, as far as hematoxylin is considered, its specific quantum yield is not known, so the same procedure provides the values of the so-called action cross-section [23]. The final results are shown in Figure 8, where the absolute TPA cross-sections of eosin and hematoxylin are displayed at several wavelengths and concentrations in water solution.

These data demonstrate the reliability of the LSTPM setup to suitably assess the TPA properties of a given sample. Particularly, the proposed technique is able to overcome the low signal-to-noise ratio of TPA measurements, which is often regarded as one of the main issues of such a kind of measurements [7]. This makes the proposed method very promising for the development of relatively easy and cheap setups for nonlinear absorption characterization.

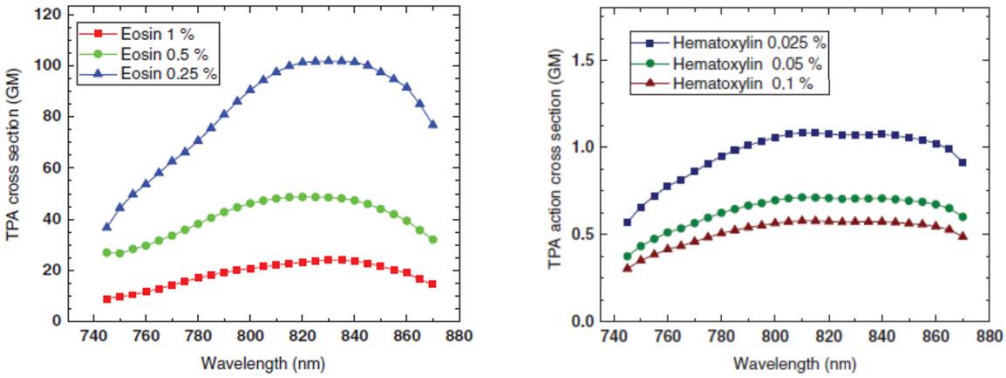

(**a**) (**b**)

Figure 8. Adapted from [14]. Measured two-photon absorption cross-section of (**a**) eosin in water solution at 1% (red), 0.5% (green), and 0.25% (blue) concentrations, and (**b**) hematoxylin in water solution at 0.1% (red), 0.05% (green), and 0.025% (blue) concentrations. Reproduced with permission from the authors, J. Microsc.; published by Wiley, 2018.

3.3. Imaging of Biological Samples

As far as imaging is concerned, the performance of the microscope setup has been tested with several biological samples. As a first example, we report results about murine macrophage-like RAW 264.7 cells incubated with lipoprotein(a), whose related morphological changes are studied. As lipoprotein(a) is well-known to be a genetic risk factor for atherosclerotic diseases, but its pathogenic mechanism is not completely clear, it is very interesting to highlight its internalization by cells. For this investigation, we have employed a 60× objective with a 1.4 numerical aperture so that the field of view is 150 × 112 μm^2. The excitation wavelength was 830 nm and the average power impinging on the sample was 60 mW. The cells were stained with Nile red and they generated no fluorescence signal when they were not treated. On the other hand, a strong signal upon two-photon excitation could be easily detected following incubation, as the image in Figure 9 clearly shows. Interestingly, we observed that lipids tended to accumulate throughout the cells, and especially in the middle part.

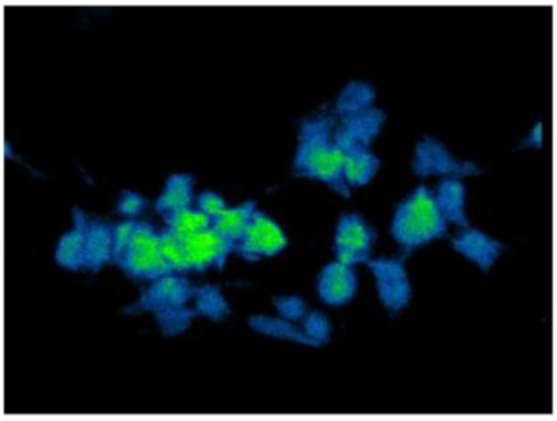

Figure 9. Adapted from [17]. Green fire and blue coloring of Nile red-stained cells: the picture underlines high-density accumulation (fire-green zones) versus low-density accumulation of fluorescence.

As a second example, we present images of mouse ovarian follicles stained with eosin and hematoxylin. Several samples have been sectioned from the same tissue and differently prepared to investigate the role of each dye and their mutual interactions. The experimental parameters were the same except for the average excitation power, which was set at 100 mW. In Figure 10, images from the following specimens are presented: eosin-stained (A), hematoxylin-stained (B), first eosin- and then hematoxylin-stained (C),

and first hematoxylin- and then eosin-stained (D). When drawing a comparison between the images of the two samples stained with either of the two dyes, it was clear that the eosin-stained sample provided a much higher two-photon fluorescence level than the hematoxylin-stained sample, as it was to be expected based on the different values of the cross-sections presented in the previous section. More interestingly, when the different regions from which the signal was generated were analyzed, it could be seen that eosin bound mostly to the nucleus and the follicle epithelium, while hematoxylin bound mostly to the zona pellucida.

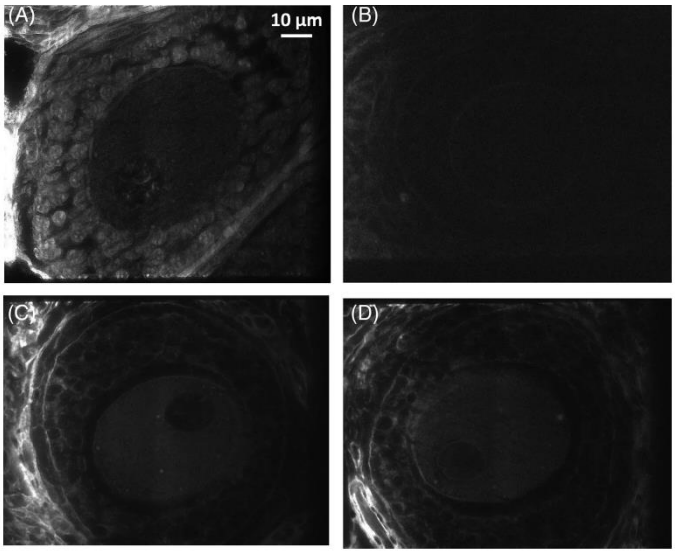

Figure 10. Adapted from [14]. Pictures of mouse ovary cells stained with either eosin or hematoxylin. (**A**) Sample stained with eosin only, (**B**) sample stained with hematoxylin only, (**C**) sample stained first with eosin and then with hematoxylin, and (**D**) sample stained first with hematoxylin and then with eosin. Reproduced with permission from the authors, J. Microsc.; published by Wiley, 2018.

The two images of the counterstained specimens thus provided greater detail (see Figure 10). The reduced signal level with respect to the eosin-stained sample is an indication of quenching phenomena arising from the interaction of the two chromophores. The almost identical images suggest that the order in which the specimens are stained with the two dyes does not play any major role.

The maximum speed of imaging that we could achieve was 96 frames/s, corresponding to the limit of the camera used in the described measurements. However, preliminary tests carried out with faster devices have demonstrated frame rates up to 350 frames/s. The improvement with respect to two-photon point-scanning microscopes which can acquire no more than a few images per second is clear, and appears to be very promising for the investigation of dynamic processes in biology and life sciences.

3.4. In-Depth Sample Reconstruction

One of the key features of two-photon microscopy is the capability of imaging at deep positions inside highly scattering media, which is the case when investigating biological samples. In this regard, the performance of our LSTPM setup has been tested. An example is provided in Figure 11, which shows the three-dimensional reconstruction of a 100 µm-thick sample of a nevus obtained by a stack of 70 two-dimensional images which have not been processed. Additionally, for this investigation, we have employed a 60× objective with a 1.4 numerical aperture. The excitation wavelength was 800 nm and the average power impinging on the sample was 50 mW. The very good quality of such raw image even down to several tens of micrometers is clear proof not only of the penetration depth of our microscope setup, but also of its axial resolution, which turned out to be comparable to the resolution of point-scanning systems. The measured axial resolution was 1.2 µm for

such experimental parameters. By drawing a comparison with the results reported in [10], we note that our LSTPM yields a better resolution with no need for control of the temporal profile of the excitation pulse.

Figure 11. Adapted from [16]. Three-dimensional reconstruction of a nevus. Reproduced with permission from the authors, proceedings of International Conference on BioPhotonics; published by IEEE, 2019.

4. Conclusions

In this paper, we have provided a brief overview of the applications of an innovative *line-scanning two-photon microscope* setup. By means of a properly optimized optical design, the usual drawbacks of such a kind of configuration were basically overcome, yielding a performance comparable to standard point-scanning microscopes. The optical setup has been experimentally demonstrated to be able to efficiently investigate spectral features and cross-sections of dyes, to accomplish imaging of biological tissues and in-depth sample reconstruction. A very good performance was recorded in every case, confirming the great flexibility and good reliability of the proposed approach. We thus believe that further developments can turn out to be successful for future applications in the field of nonlinear microscopy. Particularly, we are currently investigating the use of our setup for in vivo investigation of cancers.

5. Patents

Several concepts of the described microscopy apparatus are reported in the European Patent application of [12].

Author Contributions: All authors contributed equally. All authors have read and agreed to the published version of the manuscript.

Funding: This work was partially funded by CrestOptics.

Institutional Review Board Statement: Not applicable.

Informed Consent Statement: Not applicable.

Data Availability Statement: The paper is entirely based on previously published papers and proceedings.

Acknowledgments: We dedicate this work to the dear memory of our colleague, teacher, and friend Alessandra Tomaselli, who made an essential contribution in conceiving, developing, and testing the presented microscopy setup.

Conflicts of Interest: The authors declare no conflict of interest.

References

1. So, P.T.C.; Dong, Y.C.; Masters, B.R.; Berland, K.M. Two-Photon Excitation Fluorescence Microscopy. *Annu. Rev. Biomed. Eng.* **2000**, *2*, 399–429. [CrossRef] [PubMed]
2. Denk, W.; Strickler, J.H.; Webb, W.W. Two-photon laser scanning fluorescence microscopy. *Science* **1990**, *248*, 73–76. [CrossRef] [PubMed]
3. Berland, K.M.; So, P.T.; Gratton, E. Two-photon fluorescence correlation spectroscopy: Method and application to the intracellular environment. *Biophys. J.* **1995**, *68*, 694–701. [CrossRef]
4. Brakenhoff, G.J.; Müller, M.; Ghauharali, E.I. Analysis of efficiency of two-photon versus single-photon absorption for fluorescence generation in biological objects. *J. Microsc.* **1995**, *183*, 140–144. [CrossRef] [PubMed]
5. Schultz, S.R.; Copeland, C.S.; Foust, A.J.; Quicke, P.; Schuck, R. Advances in two photon scanning and scanless microscopy technologies for functional neural circuit imaging. *Proc. IEEE Inst. Electr. Electron. Eng.* **2017**, *105*, 139–157. [CrossRef] [PubMed]
6. Carriles, R.; Shafer, D.N.; Sheetz, K.E.; Field, J.J.; Chisek, R.; Barzda, V.; Sylvester, A.W.; Squier, J.A. Imaging techniques for harmonic and multiphoton absorption fluorescence microscopy. *Rev. Sci. Instrum.* **2009**, *80*, 081101. [CrossRef] [PubMed]
7. Rumi, M.; Perry, J.W. Two-photon absorption: An overview of measurements and principles. *Adv. Opt. Photonics* **2010**, *2*, 451–518. [CrossRef]
8. Guild, J.B.; Webb, W.W. Line scanning microscopy with two-photon fluorescence excitation. W-Pos. 192. *Biophys. J.* **1995**, *68*, A290.
9. Brakenhoff, G.J.; Squier, J.; Norris, T.; Bilton, A.C.; Wade, M.H.; Athey, B. Real-time two-photon confocal microsocopy using a femtosecond, amplified Ti:sapphire system. *J. Microsc.* **1996**, *181*, 253–259. [CrossRef] [PubMed]
10. Tal, E.; Oron, D.; Silberberg, Y. Improved depth resolution in video-rate line-scanning multiphoton microscopy using temporal focusing. *Opt. Lett.* **2005**, *30*, 1686–1688. [CrossRef] [PubMed]
11. Parravicini, J.; Tartara, L.; Hasani, E.; Tomaselli, A. Fast calculation of the line-spread-function by transversal directions decoupling. *J. Opt.* **2016**, *18*, 075609. [CrossRef]
12. Tomaselli, A.; Tartara, L.; Hasani, E. Two-Photon Excited Fluorescence Microscope. European Patent WO/2014/154279, 28 March 2013.
13. Hasani, E.; Parravicini, J.; Tartara, L.; Tomaselli, A.; Tomassini, D. Measurement of two-photon-absorption spectra through nonlinear fluorescence produced by a line-shaped excitation beam. *J. Microsc.* **2018**, *270*, 210–216. [CrossRef] [PubMed]
14. Parravicini, J.; Tomaselli, A.; Hasani, E.; Tomassini, D.; Manfredi, N.; Tartara, L. Practical two-photon-absorption cross sections and spectra of Eosin and Hematoxylin. *J. Biophotonics* **2020**, *13*, e202000141. [CrossRef] [PubMed]
15. Hasani, E.; Tartara, L.; Tomaselli, A. A novel technique for the measurement of twophoton absorption spectra of dyes for nonlinear fluorescence microscopy. In Proceedings of the 2019 IEEE International Conference on BioPhotonics (BioPhotonics), Taipei, Taiwan, 15–18 September 2019; pp. 1–3. [CrossRef]
16. Hasani, E.; Tartara, L.; Tomaselli, A. Line-scanning two-photon microscope for the investigation of biological samples. In Proceedings of the 2019 IEEE International Conference on BioPhotonics (BioPhotonics), Taipei, Taiwan, 15–18 September 2019; pp. 1–2. [CrossRef]
17. Pasquetto, M.V.; Santonastaso, A.; Tomaselli, A.; Vaghi, P.; Hasani, E.; Tartara, L.; Scotti, C. Lipoprotein (a) Internalization by RAW 264.7 Cells is Associated with Morphological Changes and Accumulation of Lipids Detectable by Two-photon Scanning Microscopy. *Br. J. Med. Med. Res.* **2016**, *17*, 1–12. [CrossRef]
18. Edelstein, A.D.; Tsuchida, M.A.; Amodaj, N.; Pinkard, H.; Vale, R.D.; Stuurma, N. Advanced methods of microscope control using μManager software. *J. Biol. Methods* **2014**, *1*, e10. [CrossRef] [PubMed]
19. μManager Official Website. Available online: https://micro-manager.org/ (accessed on 20 January 2022).
20. Sutherland, R.L. *Handbook of Nonlinear Optics*, 2nd ed.; Marcel Dekker: New York, NY, USA, 2003.
21. Zipfel2020—Two-Photon Action Cross Sections of Alexa 488 Colorant, from Zipfel Lab Online Database of Cornell University. Available online: http://zipfellab.bme.cornell.edu/ (accessed on 10 April 2020).
22. Xu, C.; Webb, W.J. Measurement of two-photon excitation cross sections of molecular fluorophores with data from 690 to 1050 nm. *Opt. Soc. Am. B* **1996**, *13*, 481. [CrossRef]
23. Cabrera, R.; Gabriel, M.; Estrada, L.C.; Etchenique, R. Direct Measurement of Two-Photon Action Cross Section. *Anal. Chem.* **2019**, *91*, 5968. [CrossRef] [PubMed]